Nuclear Materials and Energy 38 (2024) 101558

Contents lists available at ScienceDirect

Nuclear Materials and Energy

journal homepage: www.elsevier.com/locate/nme

Resonant Laser Induced Breakdown Spectroscopy for quantitative elemental depth profile analysis of WTa coating

Sahithya Atikukke [a], Matej Veis [a], Waseem Khan [b], Eduard Grigore [c], Flaviu Baiasu [c], Pavol Ďurina [a], Tomáš Roch [a], Pavel Dvořák [b], Pavel Veis [a,*]

[a] Dept. of Experimental Physics, FMPI, Comenius Univ., Mlynska dol. F2, 842 48 Bratislava, Slovakia
[b] Department of Physical Electronics, Faculty of Science, Masaryk University, Kotlarska 2, Brno 611 37, Czech Republic
[c] NILPRP 409, 077125 Magurele, Romania

ARTICLE INFO

Keywords:
LIBS
RLIBS
CFLIBS
PFC

ABSTRACT

This work reports on the procedure of Resonant-LIBS, in which ablation and subsequent excitation is achieved by fine-tuning an Optical Parametric Oscillator (OPO) laser to the resonant transition of tungsten (W I) at 255.14 nm and analyzing the optical emission spectroscopy results. Compared to conventional LIBS, the ablation rate is significantly reduced in the resonant regime, resulting in finer resolution of depth profiles. This reduction in ablation rate can be attributed to a process called Resonance Laser Ablation (RLA) where a part of the laser energy is employed for ablation, while the rest is dedicated to resonant excitation. The sample under consideration is a WTa-coated (7μm) Mo substrate prepared by a dual magnetron sputtering system. These efforts are motivated by the need for improvement in quantitative depth analysis of W-based Plasma-Facing Components (PFC). Particularly to target the undesirable surface modifications due to the interaction with H isotopes in fusion plasma, such as fuel retention or erosion/deposition.

1. Introduction

Laser-Induced Breakdown Spectroscopy (LIBS) finds niche applications in fusion technology for elemental analysis of surface layers formed due to sputtering, migration, and redeposition of wall material from various sources, including impurities and fuel retention, the sustainable operation of thermonuclear reactor and adherence to nuclear safety regulations require the control of wall composition, including the quantification of retained fuel (D/T) [1–3]. This control should be conducted in situ through remote analysis with the assistance of a robotic arm system on-site [4]. LIBS stands out as the best available technique for this purpose. The composition of the deposited layer on the Plasma Facing Materials (PFM), which includes retained fuel, ranges from the nano-meter scale (fuel retention) to several micro-meters or more (redeposited layer) [5], hence in-depth analysis of the deposited laser is necessary.

In the case of depth profiling of thin films, the depth resolution is severely affected by the high ablation rate [6]. Hence it is necessary to reduce the ablation rate to improve depth resolution. In this work depth resolution is improved by employing Resonant Laser Induced Breakdown Spectroscopy (RLIBS). RLIBS addresses limitations in depth profiling by using photo-resonant ablation, where the laser wavelength is tuned to match the resonance absorption of one of the analytes present in the sample matrix [7–14]. In RLA, the leading edge of the laser pulse is used for ablation and the trailing edge of the same laser pulse is used for resonant excitation [10,11]. In the first phase of the laser pulse, the standard laser ablation occurs, while the trailing part of the laser pulse discriminatively excites, ionizes and heats the electrons (via inverse Bremsstrahlung) the species in accordance with the resonance wavelength of the laser used [11]. This results in a reduced ablation rate, in contrast to conventional Laser-Induced Breakdown Spectroscopy (LIBS) with lasers operating at 1064 nm or 532 nm wavelengths, as only a fraction of the laser energy is employed for the ablation process. Tungsten is considered as a noble metal due to its high melting point (3680 K), low sputtering yield, and high thermal conductivity (150 W/mK). Therefore, materials based on tungsten are most likely to be used in the divertor of ITER [15]. However, the ductile to brittle transition temperature (DBTT) for W-alloys falls between 423 K and 673 K, causing brittleness when cooled with water. When tungsten is employed as the PFM, it surpasses the creep temperature limit and reaches a

* Corresponding author.
E-mail address: pavel.veis@fmph.uniba.sk (P. Veis).

https://doi.org/10.1016/j.nme.2023.101558
Received 10 August 2023; Received in revised form 14 November 2023; Accepted 15 November 2023
Available online 18 November 2023

recrystallization temperature at 1300 K. Voids in the isotropic cubic crystal structure of tungsten easily trap and retain hydrogen isotopes, causing thermal diffusion of impurities into the material. Tungsten exhibits a high energy threshold for physical sputtering with deuterium (D) and tritium (T) compared to low Z materials. Conversely, the sputtering rate significantly rises with heavier atoms, exceeding unity approximately at 770 K. Furthermore, tungsten is vulnerable to chemical erosion in the presence of oxygen. Chemically active impurity atoms ionize, forming multiply charged ions that collide with PFCs at an increased velocity, increasing the likelihood of erosion [16–19]. Considering these issues withW, we have opted to use a laser wavelength that aligns with the resonant excitation of tungsten (W I spectral line at 255.14 nm) for ablation to study erosion, migration of impurities and fuel retention.

2. Experimental setup

The depth profiling via RLIBS is done by a ns tuneable laser at atmospheric pressure in an open environment. The EKSPLA NT342C, an integrated laser system that combines a tuneable nanosecond OPO with an Nd:YAG Q-switched nanosecond laser is employed for ablation. The laser can be tuned from 210 to 2600 nm. The maximum laser pulse energy is 50 mJ (visible range) and 10 mJ (UV). The pulse duration of the laser is 3-5 ns, and pulse repetition rates are up to 30 Hz. The sample under study contains a tungsten and tantalum coating on a molybdenum substrate (W-Ta 19 at.%), hence the laser wavelength is tuned to the resonant W I transition. The excitation wavelength was chosen to be 255.14 nm under resonant conditions and 222.75 nm under off-resonant conditions. The laser was focused onto the sample by a UV-grade fused silica plano-convex lens (focal length 5 cm) for laser ablation. The OES signal from the LIBS plume was collected by a quartz optical fibre into an echelle spectrometer (ME5000, Andor Tech, detection range 200–900 nm, resolving power 4000). The spectrometer is equipped with an iCCD camera (iStar DH743, Andor Tech) with a temporal resolution of 5 ns. The depth profiling is recorded as a kinetic series of 150 consecutive laser pulses at one location, and the same procedure is performed at six various locations on the sample for averaging. The energy of the laser was set to 2 mJ for both resonant and off-resonant conditions, which is just above the ablation threshold for the sample under investigation. The optimal gate delay and gate width were identified as 500-500 ns and 1000-1000 ns, respectively, under conditions that best satisfied the requirements for Calibration-Free LIBS (CF LIBS). The spectra are divided by the sensitivity curve, and the spectral lines are identified using NIST and Kurucz spectral databases [20,21]. The ablation rates were analyzed using 3D laser scanning confocal microscopy (Keyence VK-X). The experimental setup is depicted in Fig. 1.

3. Results

From the LIBS spectra of the coated layer, a significant quantity of lines from both neutral and singly ionized Wand Ta elements have been identified for the purpose of quantification. A set of lines free from interference and self-absorption are chosen to calculate electron temperature using Boltzmann plots as shown in Fig. 2 and Fig. 3 for the spectrum recorded at delay and gate width of 1000 ns. The depth profile with 150 laser shots is plotted in Fig. 4 and Fig. 5 at resonant and off-resonant conditions, both cases using 2 mJ per laser pulse. The depth profiles reveal that at the off-resonant condition, reaching the Mo substrate requires approximately 30 laser shots, whereas, at the resonant condition, it necessitates 90 laser shots to reach the substrate, thus demonstrating that RLIBS offers higher depth resolution compared to conventional LIBS. The ablation rate is found to be 0.09 μm/pulse at resonance and 0.248 μm/pulse at the off-resonant condition through 3D laser scanning confocal microscopy. Consequently, the depth of the WTa-coating is calculated to be 7.67 μm and 6.18 μm for resonant and off-resonant conditions, respectively. The variation in the determined thickness under the two conditions may be attributed to the non-uniform coating, as ablation for resonant and off-resonant conditions was performed at different locations on the same sample. The depth of the coated layer was also calculated via the Glow Discharge Optical Emission Spectroscopy (GDOES) method on the reference sample (on a Ti substrate) deposited simultaneously with the studied samples, yielding a

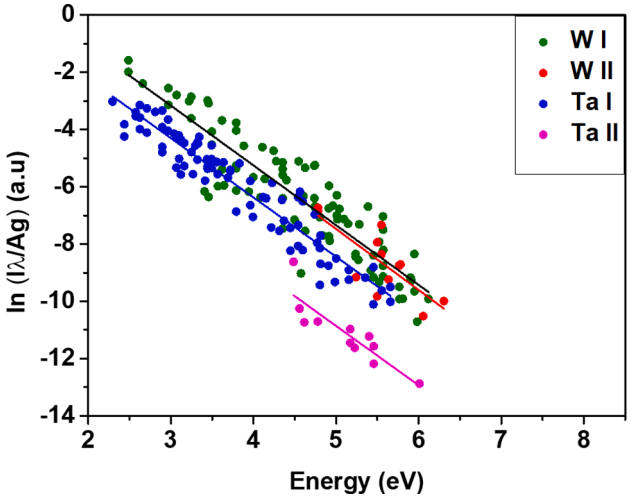

Fig. 2. Boltzmann plots at resonant conditions at gate delay and width 1000 ns.

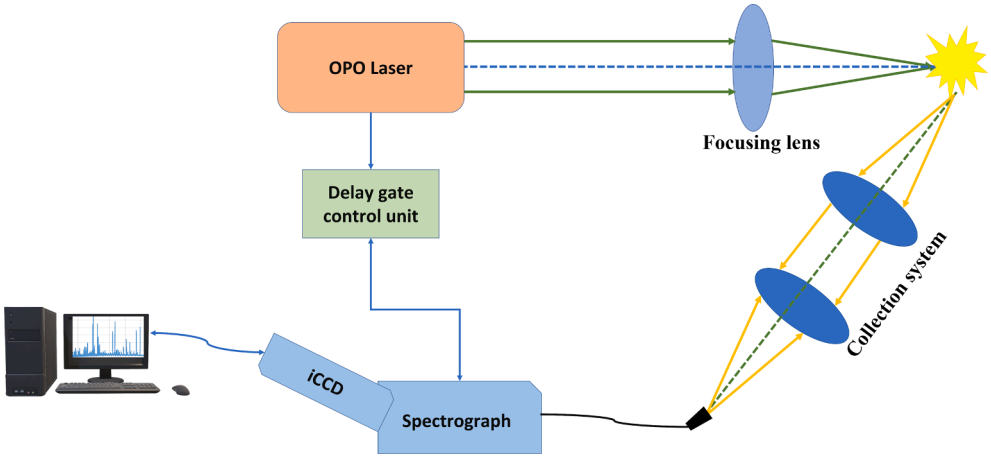

Fig. 1. Schematic diagram of the experimental setup.

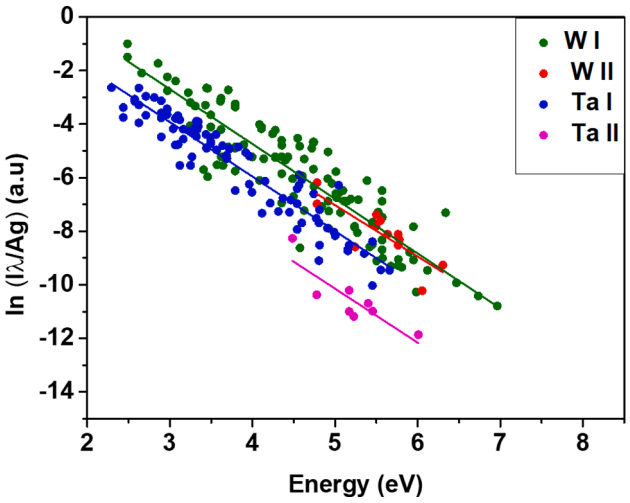

Fig. 3. Boltzmann plots at off-resonant conditions at gate delay and width 1000 ns.

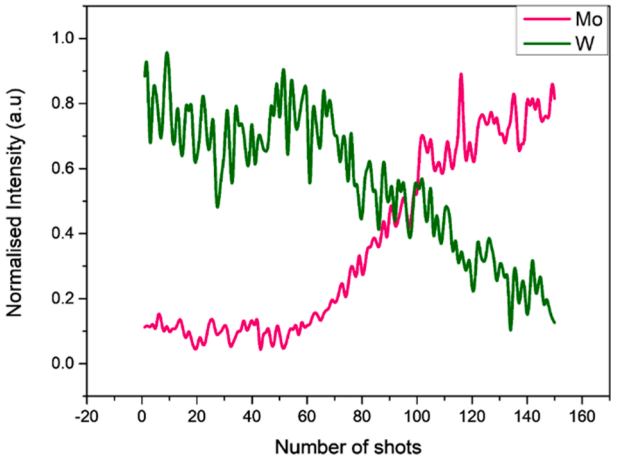

Fig. 4. Depth profile at resonance condition.

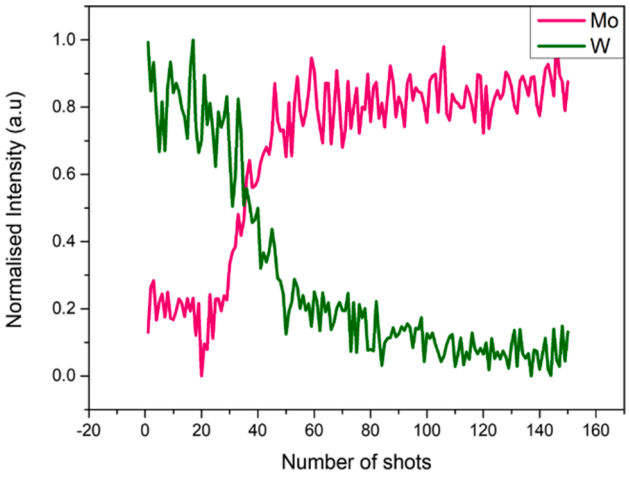

Fig. 5. Depth profile at off-resonant conditions.

value of approximately 7 μm. This result confirms the validity of depth evaluation using the combination of LIBS and interferometry. The depth profile obtained by GDOES on Ti samples is shown in Fig. 6. The elemental composition of the coated layer is done by CF LIBS which is

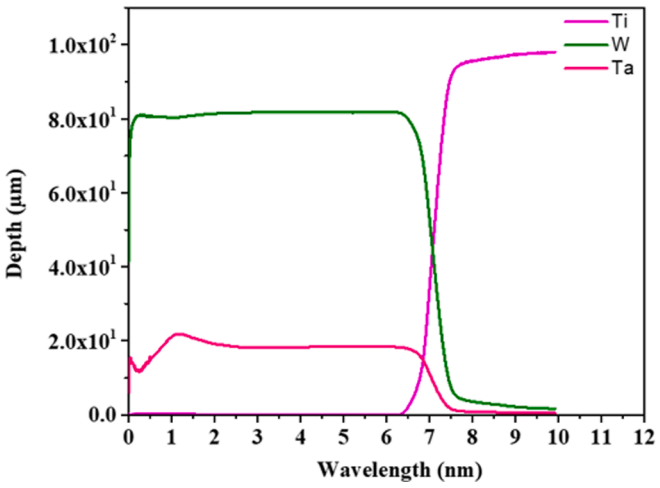

Fig. 6. Depth profile by GDOES.

well described by Ciucci et al. [22]. CF LIBS has become a well-established method in nuclear fusion for quantifying first wall elemental composition including D/T fuel retention, see [23–26]. In this work, the CF LIBS quantification, and electron density was determined using the Saha equation. The average electron temperature, which showed comparable values across all tungsten and tantalum species, was used in the specified calculation. The electron density and electron temperature have been tabulated in Table 1 and Table 2 at resonant and off-resonant conditions, respectively. From Table 1 and Table 2, it is evident that under resonant conditions, the electron density is notably low, and hence the plasma is optically thinner compared to the off-resonant conditions. The assessed electron temperature is nearly identical in both instances. The elemental quantification by CF LIBS is tabulated in Table 3 and 4, respectively. The nominal composition of the coated layer consists of 81% tungsten (W) and 19% tantalum (Ta). The elemental composition obtained through LIBS analysis is in good agreement with the specified nominal composition.

4. Conclusion

This study involves a detailed analysis of a WTa coated sample on a Mo substrate using RLIBS. A comparison was made between the ablation rate achieved at resonant conditions in RLIBS and conventional LIBS at off-resonant conditions. The results showed that the ablation rate was approx. three times lower at resonant condition compared with the off-resonant condition. This difference can be attributed to the fact that, during resonance conditions, a portion of the laser energy is utilized for ablation while the remaining energy is used for resonant excitation. In the recorded spectra, the signal intensity obtained at resonant conditions was comparable to that recorded at off-resonant conditions, despite the significantly smaller quantity of material being ablated at resonant conditions. Hence, the precision of the CF LIBS quantification was at the same level at the rate of less ablation in resonant conditions. Consequently, the depth resolution was significantly improved through RLIBS. It should be noted that, under resonant conditions, the electron density is considerably lower than at off-resonant conditions, resulting in an optically thin plasma. Although the Local Thermodynamic Equilibrium is only partially satisfied since the laser energy is just slightly above the threshold, the depth of the WTa-coated layer was determined

Table 1
Electron temperature and density measured at resonant conditions.

Resonance/Delay	T_e (eV)	$n_e(10^{15}$ cm$^{-3})$
500 ns	0.513 ± 0.047	0.50 ± 0.15
1000 ns	0.478 ± 0.053	0.16 ± 0.035

Table 2
Electron temperature and density measured at off-resonant conditions.

Non-Resonance/Delay	T_e (eV)	$n_e(10^{15}$ cm$^{-3})$
500 ns	0.546 ± 0.047	1.15 ± 0.29
1000 ns	0.500 ± 0.052	0.35 ± 0.1

Table 3
Quantification on WTa coating at resonant conditions.

Resonance/Delay	**500 ns**	**1000 ns**
W (at %)	80.80 ± 1.40	80.80 ± 2.00
Ta (at %)	19.20 ± 1.20	20.00 ± 2.00

Table 4
Quantification on WTa coating at off-resonant conditions.

Non-Resonance/Delay	**500 ns**	**1000 ns**
W (at %)	80.80 ± 1.50	80.10 ± 1.80
Ta (at %)	19.20 ± 1.50	19.90 ± 1.80

to be approximately 7.67 μm and 6.18 μm at resonant and off-resonant conditions, respectively, which closely matched the depth calculated using GDOES. Additionally, the elemental composition was quantitatively determined and found to be in close agreement with the expected composition. RLIBS demonstrated enhanced depth resolution compared to conventional LIBS.

CRediT authorship contribution statement

Sahithya Atikukke: Methodology, Formal analysis, Investigation, Writing – original draft, Visualization. **Matej Veis:** Writing – review & editing, Visualization. **Waseem Khan:** Investigation. **Eduard Grigore:** Resources, Writing – review & editing. **Flaviu Baiasu:** Resources, Writing – review & editing. **Pavol Durina:** Resources, Writing – review & editing. **Tomáš Roch:** Resources, Writing – review & editing. **Pavel Dvořák:** Investigation. **Pavel Veis:** Conceptualization, Methodology, Formal analysis, Visualization, Supervision, Writing – review & editing.

Declaration of Competing Interest

The authors declare that they have no known competing financial interests or personal relationships that could have appeared to influence the work reported in this paper.

Data availability

Data will be made available on request.

Acknowledgement

This work has been carried out within the framework of the EUROfusion Consortium, funded by the European Union via the Euratom Research and Training Programme (Grant Agreement No 101052200 - EUROfusion). Views and opinions expressed here are however those of the author(s) only and do not necessarily reflect those of the European Union or European Commission. Neither the European Union nor the European Commission can be held responsible for them. The authors acknowledge the Scientific Grant Agency of the Slovak Republic (contract numbers- VEGA 1/0803/21, VEGA 2/0144/21), the Slovak Research and Development Agency (APVV-16-0612 and APVV-22-0548), and Grant UK (UK/201/2023) for financial support. This research has been supported by Project LM2018097 funded by the Ministry of Education, Youth and Sports of the Czech Republic.

Dedication

This work is dedicated in memory of the hundredth birth anniversary of Prof. Štefan Veis, DrSc. (* December 5, 1923, Ilija – † April 22, 1981, Bratislava), a distinguished pioneer in plasma physics in Czechoslovakia.

References

[1] H. Van Der Meiden, S. Almaviva, J. Butikova, V. Dwivedi, P. Gasior, W. Gromelski, A. Hakola, X. Jiang, I. Jõgi, J. Karhunen, et al., Monitoring of tritium and impurities in the first wall of fusion devices using a LIBS based diagnostic, Nuclear Fusion 61 (12) (2021), 125001.
[2] G.S. Maurya, A. Mańın-Roldán, P. Veis, A.K. Pathak, P. Sen, A review of the LIBS analysis for the plasma-facing components diagnostics, Journal of Nuclear Materials 541 (2020), 152417.
[3] C. Li, C.-L. Feng, H.Y. Oderji, G.-N. Luo, H.-B. Ding, Review of LIBS application in nuclear fusion technology, Frontiers of Physics 11 (2016) 1–16.
[4] S. Almaviva, L. Caneve, F. Colao, V. Lazic, G. Maddaluno, P. Mosetti, A. Palucci, A. Reale, P. Gasior, W. Gromelski, et al., LIBS measurements inside the FTU vacuum vessel by using a robotic arm, Fusion Engineering and Design 169 (2021), 112638.
[5] J. Karhunen, A. Hakola, J. Likonen, A. Lissovski, M. Laan, P. Paris, J. E. Contributors, Applicability of LIBS for in situ monitoring of deposition and retention on the ITER-like wall of jet–comparison to sims, Journal of Nuclear Materials 463 (2015) 931–935.
[6] K. Novotny, T. Vaculovic, M. Galiová, V. Otruba, V. Kanicky‘, J. Kaiser, M. Liška, O. Samek, R. Malina, K. Paleniková,, The use of zinc and iron emission lines in the depth profile analysis of zinc-coated steel, Applied Surface Science 253 (8) (2007) 3834–3842.
[7] N. Cheung, Resonance-Enhanced LIBS, Fundamentals and Applications, Laser-Induced Breakdown Spectroscopy, 2006.
[8] H. Loudyi, K. Rifai, S. Laville, F. Vidal, M. Chaker, M. Sabsabi, Improving laser-induced breakdown spectroscopy (libs) performance for iron and lead determination in aqueous solutions with laser-induced fluorescence (LIF), Journal of Analytical Atomic Spectrometry 24 (10) (2009) 1421–1428.
[9] D. Cleveland, P. Stchur, X. Hou, K.X. Yang, J. Zhou, R.G. Michel, Resonant laser ablation of metals detected by atomic emission in a microwave plasma and by inductively coupled plasma mass spectrometry, Applied Spectroscopy 59 (12) (2005) 1427–1444.
[10] C. Gill, A. Garrett, P. Hemberger, N. Nogar, Selective laser ablation/ionization for Ion Trap Mass Spectrometry: Resonant Laser Ablation, Spectrochimica Acta Part B: Atomic Spectroscopy 51 (8) (1996) 851–862.
[11] C. McLean, J. Marsh, A. Land, A. Clark, R. Jennings, K. Ledingham, P. McCombes, A. Marshall, R. Singhal, M. Towrie, Resonant Laser Ablation (RLA), International Journal of Mass Spectrometry and Ion Processes 96 (1) (1990) R1–R7.
[12] K. Ledingham, I. Borthwick, R. Singhal, The characteristics of resonant laser ablation for surface analysis, Surface and Interface Analysis 18 (7) (1992) 576–578.
[13] F. Verdun, G. Krier, J. Muller, Increased sensitivity in laser microprobe mass analysis by using resonant two-photon ionization processes, Analytical Chemistry 59 (10) (1987) 1383–1387.
[14] S. Dai, L. Jin, W. Lu, R. An, L. Tai, D. Chen, Resonant laser ablation of copper and its application in microanalysis, Applied Physics A 69 (1999) S167–S169.
[15] R. Neu, J. Riesch, J. Coenen, J. Brinkmann, A. Calvo, S. Elgeti, C. Garcia-Rosales, H. Greuner, T. Hoeschen, G. Holzner, et al., Advanced tungsten materials for plasma-facing components of DEMO and fusion power plants, Fusion Engineering and Design 109 (2016) 1046–1052.
[16] Y. Ueda, J. Coenen, G. De Temmerman, R. Doerner, J. Linke, V. Philipps, E. Tsitrone, Research status and issues of tungsten plasma facing materials for ITER and beyond, Fusion engineering and design 89 (7-8) (2014) 901–906.
[17] V. Philipps, Tungsten as material for plasma-facing components in fusion devices, Journal of Nuclear Materials 415 (1) (2011) S2–S9.
[18] M. Kaufmann, R. Neu, Tungsten as first wall material in fusion devices, Fusion Engineering and Design 82 (5–14) (2007) 521–527.
[19] J. Linke, J. Du, T. Loewenhoff, G. Pintsuk, B. Spilker, I. Steudel, M. Wirtz, Challenges for plasma-facing components in nuclear fusion, Matter and Radiation at Extremes 4 (5) (2019).
[20] A. Kramida, Y. Ralchenko, J. Reader, et al., NIST atomic spectra database lines form, NIST Atomic Spectra Database (ver. 5.2)[Online] (2014).
[21] P. L. Smith, C. Heise, J. R. Esmond, et al., Atomic spectral line database from cdrom 23 of rl kurucz, URL address: http://cfa-www.harvard.edu/amdata/ampdata/kurucz23/sekur.html (ac- cessed 01.08.2023) (1995).
[22] M. Ciucci, V. Corsi, S. Palleschi, A. Rastelli, E. Salvetti, Tognoni, New procedure for quantitative elemental analysis by laser-induced plasma spectroscopy, Applied Spectroscopy 53 (8) (1999) 960–964.
[23] J. Miskovicova, M. Angus, H. van der Meiden, P. Veis,, Selection of molybdenum lines by quantitative analysis of molybdenum- zirconium-titanium alloy by CF LIBS for future fusion applications, Fusion Engineering and Design 153 (2020), 111488.
[24] A.M. Roldan, V. Dwivedi, M. Pisarcik, M. Veis, J. Miskovicova, Y. Halahovets, P. Siffalovic, M. Drzik, P. Veis, LIBS investigation of metals suitable for plasma-

facing components: Characteristics and comparison of picosecond and nanosecond regimes, Fusion Engineering and Design 172 (2021), 112898.
[25] A.M. Roldan, M. Pisarčik, M. Veis, M. Drzik, P. Veis, Calibration- Free analysis of a tungsten-based target for diagnostics of relevant fusion materials comparing picosecond and nanosecond libs, Spectrochimica Acta Part B: Atomic Spectroscopy 177 (2021), 106055.
[26] A.M. Roldan, V. Dwivedi, M. Veis, S. Atikukke, H. van der Meiden, M. Drzik, P. Veis, Quantification of hydrogen isotopes by CF-LIBS in a W-based material (WZr) at atmospheric pressure: from ns towards ps, Physica Scripta 96 (12) (2021), 124061.